nature medicine

Identification of tendon stem/progenitor cells and the role of the extracellular matrix in their niche

Yanming Bi[1], Driss Ehirchiou[2], Tina M Kilts[1], Colette A Inkson[1], Mildred C Embree[1], Wataru Sonoyama[1], Li Li[1], Arabella I Leet[3], Byoung-Moo Seo[1], Li Zhang[2], Songtao Shi[1,4] & Marian F Young[1]

The repair of injured tendons remains a great challenge, largely owing to a lack of in-depth characterization of tendon cells and their precursors. We show that human and mouse tendons harbor a unique cell population, termed tendon stem/progenitor cells (TSPCs), that has universal stem cell characteristics such as clonogenicity, multipotency and self-renewal capacity. The isolated TSPCs could regenerate tendon-like tissues after extended expansion *in vitro* and transplantation *in vivo*. Moreover, we show that TSPCs reside within a unique niche predominantly comprised of an extracellular matrix, and we identify biglycan (Bgn) and fibromodulin (Fmod) as two critical components that organize this niche. Depletion of Bgn and Fmod affects the differentiation of TSPCs by modulating bone morphogenetic protein signaling and impairs tendon formation *in vivo*. Our results, while offering new insights into the biology of tendon cells, may assist in future strategies to treat tendon diseases.

Tendons are specialized tissues that connect bone to muscle, transmitting the forces generated by these structures to allow for body movement. Tendon injuries due to overuse or age-related degeneration are a common clinical problem. Damaged tendon tissue heals very slowly and rarely attains the structural integrity and mechanical strength of normal, undamaged tendon[1]. The development of new treatment options for injured tendons has been hindered by a limited understanding of basic tendon biology[1].

The primary unit of tendon is a fiber comprised of collagen fibrils that cross-link to each other in a staggered fashion[2]. Tendon cells reside between long, parallel chains of these fibrils and synthesize a unique extracellular matrix (ECM) that contains primarily collagens, large proteoglycans and small, leucine-rich proteoglycans, which function as lubricators and as organizers for collagen fibril assembly[2,3]. Despite the large abundance of the ECM in tendon, very little is known about its role in regulating the function of the cells that reside within it. A better understanding of the mechanisms that regulate the function and the differentiation of tendon cells is essential to developing new treatments for tendinopathy such as tendon rupture or ectopic ossification resulting from injury caused by overuse or trauma.

Several lines of evidence suggest that multipotential stem cells are present in tendons and ligaments. First, both human and mouse tendons develop fibrocartilage and ossification in response to injury[4]. Second, tendon-derived immortalized cell lines or human tendon-derived fibroblasts express genes of adipogenic, osteogenic and chondrogenic differentiation pathways, suggesting that they possess multiple differentiation capacities *in vitro*[5,6]. Finally, postnatal stem cells capable of differentiating into adipocytes and osteoblastic cells have been identified in human periodontal ligaments[7]. Nevertheless, no studies to date have identified a definitive stem or progenitor cell population in tendon tissues or examined the nature of the niche that regulates the self-renewal and differentiation of tendon stem cells. The goal of our study was to determine whether adult tendon tissues harbor cells with stem-cell character and to identify critical components of the tendon stem-cell niche. We isolated a rare cell population from both human and mouse tendons and showed that they possess several universal criteria of stem cells, including clonogenicity, self-renewal and multipotent differentiation capacity. However, the cells of this population showed heterogeneity in these properties and could conceivably contain tendon progenitor cells. We therefore named these cells tendon stem/progenitor cells (TSPCs). Furthermore, we showed that TSPCs reside within a niche composed primarily of an ECM, which is unique among the known stem cell niches, including the bulge niche for skin stem cells[8], the osteoblast niche for hematopoietic stem cells[9–11] and the perivascular niche for neural stem cells and bone marrow stromal stem cells[12–14]. Finally, using genetically engineered mice, we identified Bgn and Fmod as two critical components of the tendon stem cell niche, which in turn controls the fate of tendon TSPCs in part by modulating bone morphogenic protein (BMP) activity.

RESULTS

Tendon-derived cells possess clonogenic capability

The commonly used criteria that define stem cells are clonogenicity, multipotency and self-renewal. To characterize whether

[1]Craniofacial and Skeletal Diseases Branch, National Institute of Dental and Craniofacial Research, US National Institutes of Health, 30 Convent Dr. 30/225 MSC 4320, Bethesda, Maryland 20892, USA. [2]Center for Vascular and Inflammatory Diseases, Department of Physiology, University of Maryland School of Medicine, 800 W. Baltimore Street, Baltimore, Maryland 21201, USA. [3]Division of Pediatric Orthopaedics, Johns Hopkins University, 601 N. Caroline Street, Baltimore, Maryland 21287, USA. [4]Center for Craniofacial Molecular Biology, University of Southern California School of Dentistry, 2250 Alcazar Street, CSA 103, Los Angeles, California 90033, USA. Correspondence should be addressed to M.F.Y. (myoung@dir.nidcr.nih.gov) or S.S. (songtaos@usc.edu).

Received 25 January; accepted 10 July; published online 9 September 2007; doi:10.1038/nm1630

tendon-derived cells are clonogenic, we generated and cultured single-cell suspensions from WT C57BL/6 mouse patellar tendon or human hamstring tendon. A portion of tendon-derived cells attached onto the plate and remained quiescent for 5–6 d before they started rapidly dividing to form colonies. After 8–10 d, colonies that had formed from single cells were visualized using methyl violet staining (**Fig. 1a** and **Supplementary Fig. 1a** online). A small population (~3–4%) of tendon-derived cells from both mouse and human tissue formed adherent cell colonies (**Fig. 1a**). These colonies were heterogeneous in size and cell density, potentially reflecting differences in the rate of cell proliferation (**Fig. 1a**). Morphologically, five different colony types were observed in mouse tendon-derived cell cultures (mTSPCs 1–5, **Supplementary Fig. 1b**) and they were different from bone marrow stromal cells (BMSCs, **Supplementary Fig. 1b**). Human tendon-derived cells (TSPCs) were relatively homogeneous and similar to human BMSCs (BMSCs, **Supplementary Fig. 1b**).

Tendon-derived cells are distinct from BMSCs

Before we tested TSPCs further for more stem cell criteria, we first compared the gene expression profile of TSPCs to that of BMSCs in order to identify TSPC-specific markers. Thus, we isolated mouse and human TSPCs and BMSCs from postnatal tendon tissues and bone

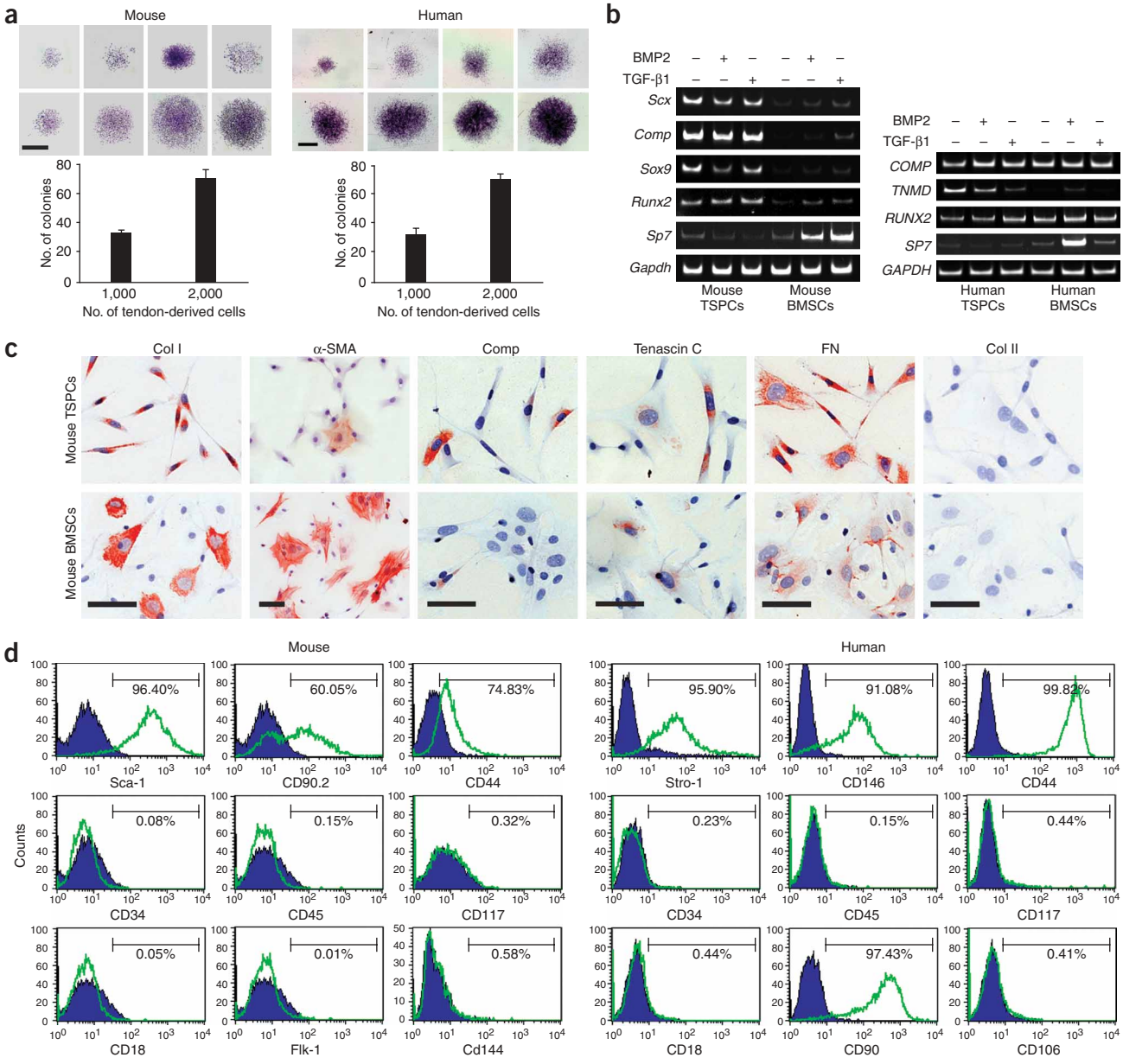

Figure 1 Isolation and characterization of TSPCs. (**a**) The colony-forming efficiency of mouse and human tendon-derived cells. The results shown are mean ± s.e.m. of 3–4 flasks. Bars, 2 mm. (**b**) RT-PCR analysis of gene expression profiles related to tendon, cartilage and bone in mouse (left) or human (right) TSPCs and BMSCs that were cultured in the presence or absence of 100 ng/ml BMP2 or 2 ng/ml TGF-β1 for 7 d. (**c**) Immunocytochemistry staining of proteins related to tendon and cartilage in mouse TSPCs and BMSCs. Bars, 50 μm. (**d**) Flow cytometry analysis of the expression of cell surface markers related to stem cells, BMSCs, hematopoietic stem cells and endothelial cells on mouse (left) and human (right) TSPCs.

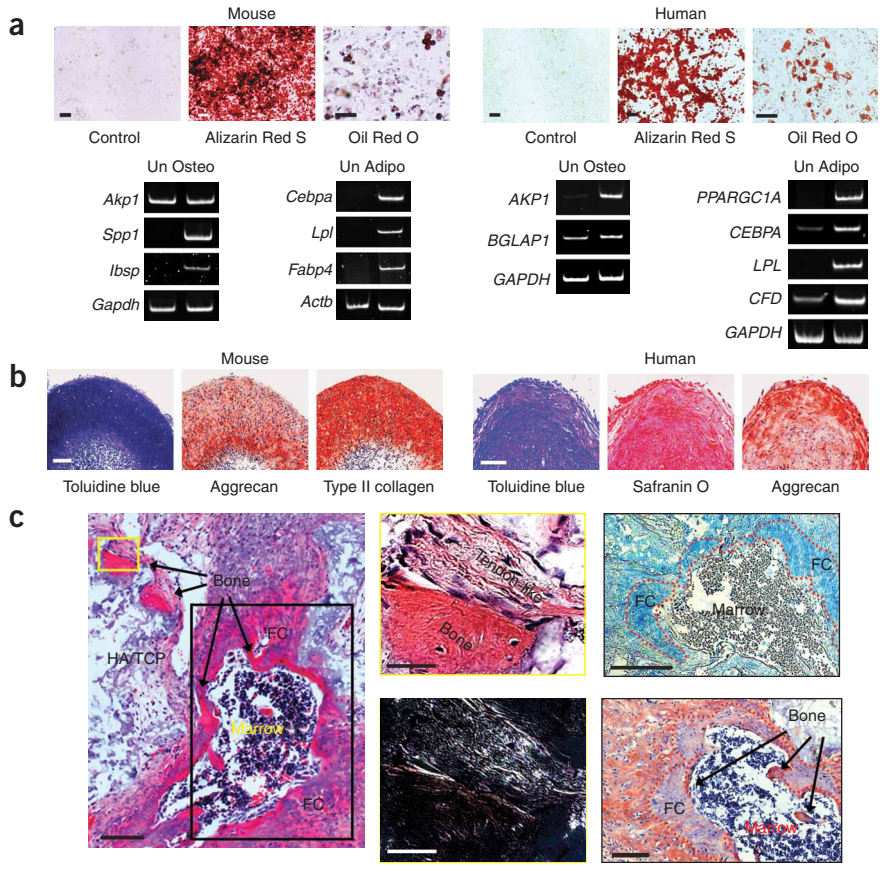

Figure 2 Multidifferentiation potential of putative mouse and human TSPCs *in vitro* and *in vivo*. (**a**) Alizarin Red S and Oil Red O staining showed osteogenic and adipogenic differentiation, respectively, of mouse (left) and human (right) TSPCs. Bar, 100 μm. RT-PCR showed gene expression profiles related to osteogenic (osteo) and adipogenic (adipo) differentiation compared to uninduced (un) cultures. (**b**) Chondrogenic differentiation of mouse (left) and human (right) TSPCs. Chondrogenic differentiation was assessed by toluidine blue, Safranin O and the expression of aggrecan and type II collagen. Bar, 100 μm. (**c**) Multipotential differentiation of mouse TSPCs *in vivo*. H&E stained sections of the transplant showed that bone, bone marrow, tendon-like tissue and fibrocartilage (FC) were formed (left). Bar, 100 μm. Higher magnification of the yellow box at upper left shows the presence of bone- and tendon-like tissues by H&E staining (top middle) and by polarized light (bottom middle). Bars, 25 μm. Fibrocartilage tissues within the black box at left were shown by Alcian blue staining of the cartilage-like tissues (top right, inside the red dashed-line boxes) and by type I collagen staining (bottom right, Col I, outside of red dashed-line boxes). Bars, 100 μm.

marrow, respectively, expanded them *in vitro* and carried out mRNA isolation and assessment. Semiquantitative reverse transcriptase (RT)-PCR showed that mouse TSPCs expressed higher amounts of scleraxis (a twist-related bHLH transcription factor encoded by the gene *Scx*)[15], cartilage oligomeric protein (*Comp*)[16], the transcription factor SOX9 (*Sox9*) and the osteogenic transcription factor runt-related transcription factor 2 (*Runx2*) as compared to mouse BMSCs (**Fig. 1b**). Human TSPCs expressed higher levels of tenomodulin (*TNMD*)[17] than did human BMSCs (**Fig. 1b**). BMP2 and transforming growth factor-β1 (TGF-β1) are important growth factors in the regulation of tendon and bone formation. Therefore, we examined how TSPCs and BMSCs responded to these factors. BMP2 and TGF-β1 inhibited TSPC expression of *Scx*, *Sox9* and *TNMD* but promoted both mouse and human BMSC expression of the genes encoding the RUNX2 and SP7 (also known as osterix) proteins. *Sp7* and *SP7* were strongly induced by BMP2 in BMSCs. The expression levels of *COMP* were similar in both human TSPCs and BMSCs (**Fig. 1b**) and were not affected by BMP2 and TGF-β1 treatment.

Immunocytochemistry staining further confirmed the unique phenotype of the isolated TSPCs. Specifically, all TSPCs expressed type I collagen, whereas only a certain population of BMSCs expressed this protein (**Fig. 1c**). On the other hand, expression of α-smooth muscle actin (α-SMA) was more abundant in BMSCs than in TSPCs (**Fig. 1c**). In line with what we showed previously using RT-PCR (**Fig. 1b**), more TSPCs than BMSCs expressed Comp and tenascin C. All TSPCs and BMSCs expressed fibronectin, but none expressed type II collagen (**Fig. 1c**).

We used flow cytometric analysis to examine the presence of surface antigens on TSPCs (**Fig. 1d**). Over 96% of mouse TSPCs (passage 0) were positive for a stem cell marker, stem cell antigen-1 (Sca-1)[18–22], and over 60% of these cells were positive for the fibroblast marker CD90.2 that was not expressed by BMSCs (**Fig. 1d** and **Supplementary Fig. 1c**). They were negative for the hematopoietic stem cell markers CD34 and CD117, for the leukocyte marker CD45, and for the endothelial cell markers Flk-1 and CD144, thus verifying the lack of contaminating hematopoietic cells and endothelial cells (**Fig. 1d**). TSPCs were positive for CD44, but not CD18, a surface receptor present on BMSCs[23] (**Fig. 1d**). Similarly, human TSPCs (passage 2) were positive for BMSC markers Stro-1, CD146 (also known as Muc18 or MCAM)[24,25], CD90 and CD44, but not for CD18 (**Fig. 1d**). Like mouse TSPCs, human TSPCs did not express the hematopoietic cell markers CD34, CD45 and CD117(c-kit) or the endothelial cell marker CD106 (**Fig. 1d**).

The putative tendon stem cells are multipotent

The multidifferentiation potentials of the TSPCs toward osteogenesis, adipogenesis and chondrogenesis were determined and then compared to those of BMSCs. Mouse and human TSPCs accumulated Ca^{2+} more rapidly and formed ~4 times more nodules than BMSCs (**Fig. 2a** and **Supplementary Fig. 2a** online). RT-PCR analysis showed that the expression of the osteogenic markers osteopontin (*Spp1*), bone sialoprotein (*Ibsp*), alkaline phosphatase (*AKP1*) and osteocalcin (*BGLAP1*) was increased after osteogenic induction for 3 weeks. Alkaline phosphatase (*Akp1*) expression in mouse cells was observed both with and without osteogenic induction. Oil Red O staining of the lipid droplets within the adipocytes, an indicator of adipogenesis, was also greater in TSPCs than in BMSCs after 3 weeks of culture in adipogenic induction medium (**Supplementary Fig. 2b**). The expression of the adipogenic markers lipoprotein lipase (*Lpl/LPL*), C/EBPα (*Cebpa/CEBPA*), aP2 (*Fabp4*), adipsin (*CFD*) and PPARγ (*PPARGC1A*) was also induced after 3 weeks of adipogenic induction. Chondrogenic differentiation after induction in chondrogenic medium was assessed in pellet culture by immunostaining of type II

collagen and aggrecan expression and by toluidine blue and Safranin O staining of the proteoglycan-rich ECM (**Fig. 2b** and **Supplementary Fig. 2c**). In addition to comparing mouse TSPCs with BMSCs, we also isolated dermal fibroblasts from the same mice and found that *in vitro*, they too could be induced to accumulate Ca^{2+} and lipid droplets (**Supplementary Fig. 2a,b**). They could not, however, be induced toward chondrogenic differentiation (**Supplementary Fig. 2c**). Like human BMSCs[26], individual colonies of human TSPCs showed heterogeneous differentiation potential toward osteogenesis, adipogenesis and chondrogenesis (**Supplementary Fig. 3a** online). The majority of colonies (14 of 18 colonies from two donors) were tripotential (that is, showed all three differentiation potentials). Small percentages were bipotential (3 of 18 colonies) and unipotential (1 of 18 colonies). To determine the multidifferentiation potential of TSPCs *in vivo*, we cultured them in osteogenic induction medium in the presence of BMP2 for 2 weeks before transplanting them subcutaneously with a carrier (hydroxyapatite/tricalcium phosphate, HA/TCP) into immunocompromised mice[27,28]. After 8 weeks, bone formation was observed on the HA/TCP carrier surface (**Fig. 2c**, left), and tendon-like tissues were observed adjacent to the newly formed bones (**Fig. 2c**, top middle), which was further confirmed by the presence of unique collagen fibers when the tissue was visualized under polarized light (**Fig. 2c**, bottom middle) and by Goldner's trichrome staining (**Supplementary Fig. 4** online). Bone marrow–like structures were found at the center of the newly formed bones and were surrounded by fibrocartilages (FC, **Fig. 2c**, left), as evidenced by positive Alcian blue staining (**Fig. 2c**, top right) and negative type I collagen staining (**Fig. 2c**, bottom right).

The putative tendon stem cells are self-renewing

Both human and mouse TSPCs proliferated faster than BMSCs isolated from the same individuals (**Fig. 3a**), as judged by bromodeoxyuridine (BrdU) incorporation. Population doubling assays showed that both mouse and human TSPCs could divide for an extensive period *in vitro* (**Fig. 3b**). Population doubling of mouse TSPCs, but not of human TSPCs, was higher than that of BMSCs (**Fig. 3b**). Furthermore, TSPCs derived from individual colonies also showed high proliferation capability for an extended period of time (**Fig. 3c**).

The high doubling capacity of TSPCs suggested that they possessed self-renewing capability. To confirm this, we examined TSPCs for their clonogenic and multidifferentiation potential after serial *in vitro* and *in vivo* expansions (**Fig. 3d**). Briefly, TSPCs were isolated from green fluorescence protein (GFP)-expressing C57BL/6 transgenic mice, expanded *in vitro* and then transplanted subcutaneously with Gelfoam into immunocompromised mice. After 8 weeks, the tendon-like tissues that formed contained GFP-positive cells, indicating their donor-cell origin (**Fig. 3e**). The transplants were removed, digested and then expanded again *in vitro*. The transplant-derived GFP-positive TSPCs retained their ability to form colonies (**Fig. 3f** and **Supplementary Fig. 5a** online) with a lower colony-forming efficiency (~2%, **Fig. 3g**). Approximately 90% of the colonies were GFP

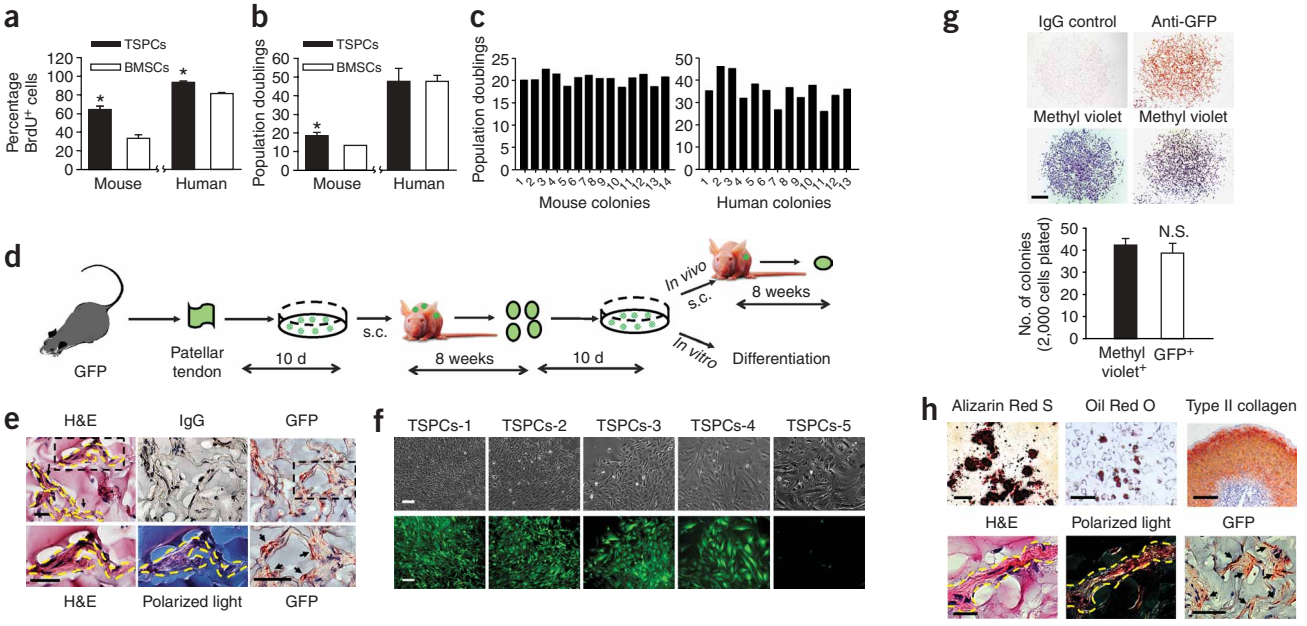

Figure 3 Self-renewal of putative tendon stem cells. (**a**) Proliferation of mouse and human TSPCs and BMSCs from the same donor measured by BrdU incorporation. Data are mean ± s.e.m. of 5–6 fields. $^*P < 0.0005$ TSPCs versus BMSCs. (**b**) Population doublings of multicolony-derived mouse and human TSPCs and BMSCs from the same donors. Data are mean ± s.e.m. of three mice or two donors. $^*P < 0.05$ TSPCs versus BMSCs. (**c**) Population doublings of single colony–derived mouse and human TSPCs. (**d**) Strategy for testing self-renewal capability of TSPCs. s.c., subcutaneous transplantation. (**e**) TSPCs from GFP-transgenic mice (arrows) formed tendon-like tissues (yellow dashed line) after being expanded *in vitro* (from 8×10^4 to 12×10^6 cells) and transplanted with Gelfoam. Bars, 25 μm. (**f**) Phase-contrast (top) and fluorescence microscopy (bottom) showed the morphology and GFP fluorescence of the colonies formed from transplant-derived cells. Bars, 200 μm. Numbers denote morphologically different types of colonies. (**g**) The colonies were stained with GFP-specific antibody (GFP; IgG as a negative control; methyl violet staining shows the total amount of colonies). Bar, 500 μm. Bottom graph shows the number of total colonies (methyl violet–stained) and GFP-positive (GFP^+) colonies. N.S., not significant total colonies versus GFP^+ colonies. (**h**) Transplant-derived TSPCs maintained their multidifferentiation capacity toward osteogenesis (Alizarin Red S; bar, 500 μm), adipogenesis (Oil Red O; bar, 200 μm) and chondrogenesis (type II collagen–positive; bar, 200 μm) *in vitro* and tendon formation (polarized light, yellow dashed line; bar, 25 μm) by GFP^+ cells (arrows) *in vivo* after being expanded *in vitro* (from 9×10^4 to 4×10^6 cells).

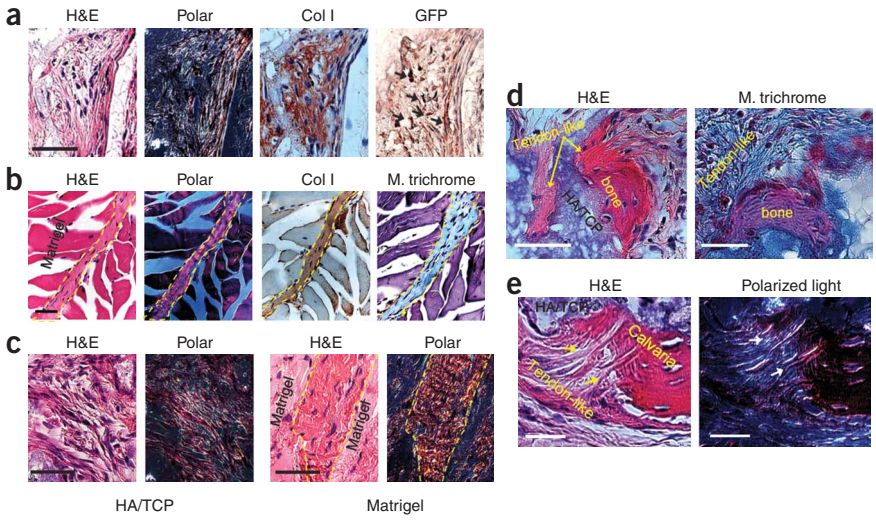

Figure 4 Regeneration potential of TSPCs. (**a**,**b**) Mouse TSPCs formed tendon-like tissue *in vivo* 8 weeks after transplantation with HA/TCP ceramic powder (**a**) or Matrigel (**b**). Tendon-like tissues were identified under polarized light (polar) or by Masson's trichrome and type I collagen staining (Col I, brown color). The origin of the tendon-like tissues was identified by GFP-specific antibody staining (black arrow). Bars, 50 μm. (**c**) Human TSPCs formed tendon-like tissue *in vivo* 8 weeks after transplantation with HA/TCP (left) and Matrigel (right). Bars, 50 μm. (**d**) Mouse BMP2–treated TSPCs formed bone-tendon junction–like tissue *in vivo* 8 weeks after transplantation with HA/TCP. Bars, 100 μm. (**e**) Human TSPCs formed Sharpey's fibers (arrows) that were inserted into the calvarial bone after transplantation with HA/TCP on the surface of calvariae for 8 weeks. Bars, 25 μm.

positive, as determined by fluorescence microscopy (**Fig. 3f**) and by GFP-specific antibody staining (**Fig. 3g** and **Supplementary Fig. 5a**). A few GFP-negative cell clusters were observed in the culture; these came from contamination of the host tissue (**Fig. 3f**, mTSPCs-5). Morphologically, the GFP-positive cells showed heterogeneity similar to that of primary tendon-derived TSPC cultures (compare **Fig. 3f** to **Supplementary Fig. 1b**). Most importantly, the transplant-derived TSPCs retained their ability to differentiate into osteoblasts, adipocytes and chondrocytes (**Fig. 3h** and **Supplementary Fig. 5b**), as well as their ability to form tendon-like tissues *in vivo* when retransplanted with Gelfoam (**Fig. 3h** and **Supplementary Fig. 5c**). These data demonstrated that even after extended expansion *in vitro* and *in vivo*, the TSPCs still retained their clonogenic and multipotent properties and their ability to form tendon-like tissues *in vivo*, thus confirming their self-renewing potential.

The putative tendon stem cells form enthesis-like tissue

The identification of TSPCs with self-renewal capability provided us with a unique opportunity to repair and regenerate damaged or diseased tendon tissues. To test the feasibility of this approach, we first expanded GFP-expressing TSPCs *in vitro* and then transplanted them with different carriers. Tendon-like tissues were generated from mouse TSPCs with either Gelfoam, HA/TCP or Matrigel as carriers (**Fig. 3e** and **Fig. 4a**,**b**). The regenerated tendon-like tissues showed tendon-specific parallel alignments of collagen fibers, as evidenced by their ability to reflect polarized light (polar, **Fig. 4a–c**). They also stained strongly for type I collagen (**Fig. 4a**,**b**), and the donor origin of the cells within the newly formed tendons was confirmed by their positive GFP staining (**Fig. 3e** and **Fig. 4a**). Mouse dermal fibroblasts transplanted with either Gelfoam or Matrigel did not form any tissue (data not shown). Similarly, human TSPCs from the initial culture and from individual colonies could generate tendon-like tissues when transplanted with HA/TCP or Matrigel (**Fig. 4c** and **Supplementary Fig. 3b**). When mouse TSPCs were treated with BMP2 and then transplanted subcutaneously into immunocompromised mice, osteo-tendinous junction–like structures (termed entheses) were formed (**Fig. 4d**). More notably, when transplanted with HA/TCP onto the surface of mouse calvariae, human TSPCs formed condensed collagen fibers that were inserted into the bone, which were similar to Sharpey's fibers (**Fig. 4e**). These results were particularly striking, as the human TSPCs, placed into a completely heterologous environment, were still able to form tissue structures similar to those found *in vivo* in humans.

Extracellular matrix organizes the tendon stem-cell niche

The differentiation and self-renewal of stem cells are regulated by the cells' specific niche. To characterize the tendon stem-cell niche, we first localized TSPCs within their natural environment. Stem cells are quiescent, but can also be slow cycling when spurred on by such stimuli as rapid growth, regeneration of tissues and *ex vivo* explantation. We were able to label stem cells by taking advantage of their slow-cycling proliferation during the rapid growth period. We administered BrdU intraperioneally into 3-d-old pups (daily for 3 d) to label the proliferating cells. One day after this labeling procedure, approximately 40% of the cells within the patellar tendon were labeled by BrdU as a result of rapid growth of the skeletal system (**Fig. 5a**). After an extended period of time (more than 8 weeks), only cells that retained the BrdU label[29], representing stem cells, could be detected. By 14 weeks, approximately 6.1 ± 1.63% of the cells within the patellar tendon still retained BrdU (**Fig. 5a**), a percentage similar to the colony-forming efficiency of tendon-derived cells (3.68 ± 0.32% for 2,000 cells plated, $P = 0.219$; compare to **Fig. 1a**).

We found that the TSPCs resided in between the long parallel chains of collagen fibrils and were surrounded predominantly by ECM. Therefore, we predicted that the TSPC niche, if it exists, is composed primarily of various ECM components. We further theorized that alteration of the ECM composition would change the structure of the TSPC niche and thus affect the fate of TSPCs. To test this hypothesis, we studied two small proteoglycans, Bgn and Fmod, that were both highly expressed in the tendon (**Fig. 5b**). Genetic inactivation of Bgn and Fmod impairs tendon formation[30]. We found that the patellar tendon in $Bgn^{-/0}Fmod^{-/-}$ mice appeared more translucent (**Fig. 5c**), significantly thinner and more cellular than that of wild-type (WT) mice (**Fig. 5d**). In the absence of Bgn and Fmod, the collagen fibers within the tendon were disorganized, as evidenced by the large gaps within the tendon tissue and the fibers' appearance under polarized light (**Fig. 5d**). On the basis of this observation, we hypothesized that an ECM-rich niche, organized in part by Bgn and Fmod, controls the self-renewal and differentiation of TSPCs. Indeed, the number of colonies in $Bgn^{-/0}Fmod^{-/-}$ mice was significantly greater than in WT mice (**Fig. 5e**). TSPCs from

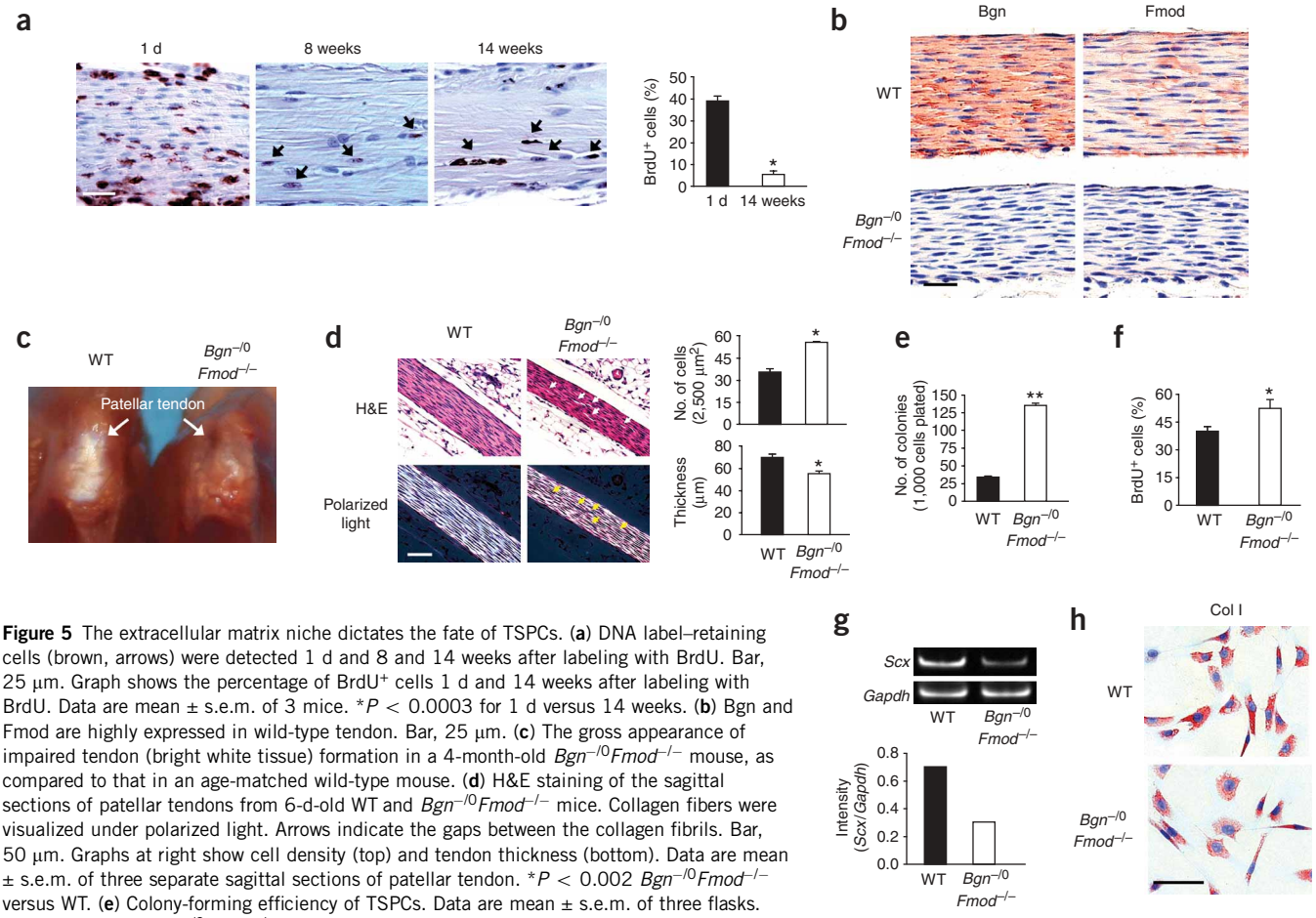

Figure 5 The extracellular matrix niche dictates the fate of TSPCs. (**a**) DNA label–retaining cells (brown, arrows) were detected 1 d and 8 and 14 weeks after labeling with BrdU. Bar, 25 μm. Graph shows the percentage of $BrdU^+$ cells 1 d and 14 weeks after labeling with BrdU. Data are mean ± s.e.m. of 3 mice. $^*P < 0.0003$ for 1 d versus 14 weeks. (**b**) Bgn and Fmod are highly expressed in wild-type tendon. Bar, 25 μm. (**c**) The gross appearance of impaired tendon (bright white tissue) formation in a 4-month-old $Bgn^{-/0}Fmod^{-/-}$ mouse, as compared to that in an age-matched wild-type mouse. (**d**) H&E staining of the sagittal sections of patellar tendons from 6-d-old WT and $Bgn^{-/0}Fmod^{-/-}$ mice. Collagen fibers were visualized under polarized light. Arrows indicate the gaps between the collagen fibrils. Bar, 50 μm. Graphs at right show cell density (top) and tendon thickness (bottom). Data are mean ± s.e.m. of three separate sagittal sections of patellar tendon. $^*P < 0.002$ $Bgn^{-/0}Fmod^{-/-}$ versus WT. (**e**) Colony-forming efficiency of TSPCs. Data are mean ± s.e.m. of three flasks. $^{**}P < 0.00002$ $Bgn^{-/0}Fmod^{-/-}$ versus WT. (**f**) Proliferation of TSPCs. Data are mean ± s.e.m. of 6–8 fields. $^*P < 0.03$ $Bgn^{-/0}Fmod^{-/-}$ versus WT. (**g**) RT-PCR shows the expression of *Scx* (top). *Gapdh*, loading control. The expression intensity was determined by densitometric analysis (bottom). (**h**) Immunocytochemistry staining of type I collagen (Col I). Bar, 50 μm.

$Bgn^{-/0}Fmod^{-/-}$ mice proliferated faster than the cells from WT mice (**Fig. 5f**). This increased number and proliferation of TSPCs may be caused by a compensation for the impaired differentiation and function of TSPCs, which could further contribute to the malformation of tendon tissue in $Bgn^{-/0}Fmod^{-/-}$ mice. This hypothesis was supported by our finding that the expression of the tendon marker *Scx* and of type I collagen was decreased in TSPCs from $Bgn^{-/0}Fmod^{-/-}$ mice as compared to cells from WT mice (**Fig. 5g,h**). Thus, the TSPC niche, formed predominantly by ECM, controls TSPC self-renewal and differentiation, and alteration of the ECM composition leads to tendon malformation and pathologic ossification.

An ECM-rich niche controls TSPC fate through BMP signaling

Human tendon tissue subjected to overuse and injures can acquire ectopic ossification[4], which might be caused by interruption of the ECM structure and, subsequently, the TSPC niche. Indeed, the impaired tendon in $Bgn^{-/0}Fmod^{-/-}$ mice underwent ossification as early as 2 months after birth and became more pronounced with age (**Fig. 6a**). Similar to intratendinous ossification in humans, ossicles formed in the tendons of $Bgn^{-/0}Fmod^{-/-}$ mice were surrounded by fibrocartilage, suggesting that ossification occurred through endochondral bone formation[4,30]. Consistent with this interpretation, we found that $Bgn^{-/0}Fmod^{-/-}$ TSPC cultures, but not WT cultures, contained type II collagen–expressing cells (**Fig. 6b**). The expression of aggrecan, a chondrocyte marker, was also increased in TSPCs in the absence of Bgn and Fmod (**Fig. 6b**). The TSPCs from $Bgn^{-/0}Fmod^{-/-}$ mice formed bone in addition to tendon-like tissue *in vivo*, whereas WT TSPCs only formed tendon-like tissue (**Fig. 6c**). We speculated that changes in TSPC niche–associated ECM composition may perturb the balance of certain cytokines and growth factors stored within the ECM and thus alter the fate of TSPCs from tenogenesis to osteogenesis. One of these regulatory cytokines is BMP2, which signals through the Smad1-Smad5-Smad-8 pathway to increase the expression of Runx2 (**Fig. 6d**) and, as a result, Ca^{2+} accumulation (**Fig. 6e**, bottom left), as measured by Alizarin Red staining, was substantially increased. Likewise, alkaline phosphatase activity (**Fig. 6e**, top left), as well as *in vivo* bone formation (**Fig. 6e**, right), were also considerably increased. Therefore, we tested whether the Smad1-Smad5-Smad8 signal transduction pathway was affected by the absence of Bgn and Fmod. Western blot analysis using a pan-pSmad antibody, showed that phosphorylation of Smad1, Smad5 and Smad8 upon treatment with BMP2 was greater in $Bgn^{-/0}Fmod^{-/-}$ TSPCs than in WT cells (**Fig. 6f**). Immunocytochemistry staining revealed more abundant nuclear localization of phosphorylated Smad1 in $Bgn^{-/0}Fmod^{-/-}$ TSPCs as compared to WT cells, and the difference was even greater after stimulation with BMP2 (**Fig. 6g**). Furthermore, transcriptional activity of a BMP-responsive luciferase reporter construct (pID-lux)

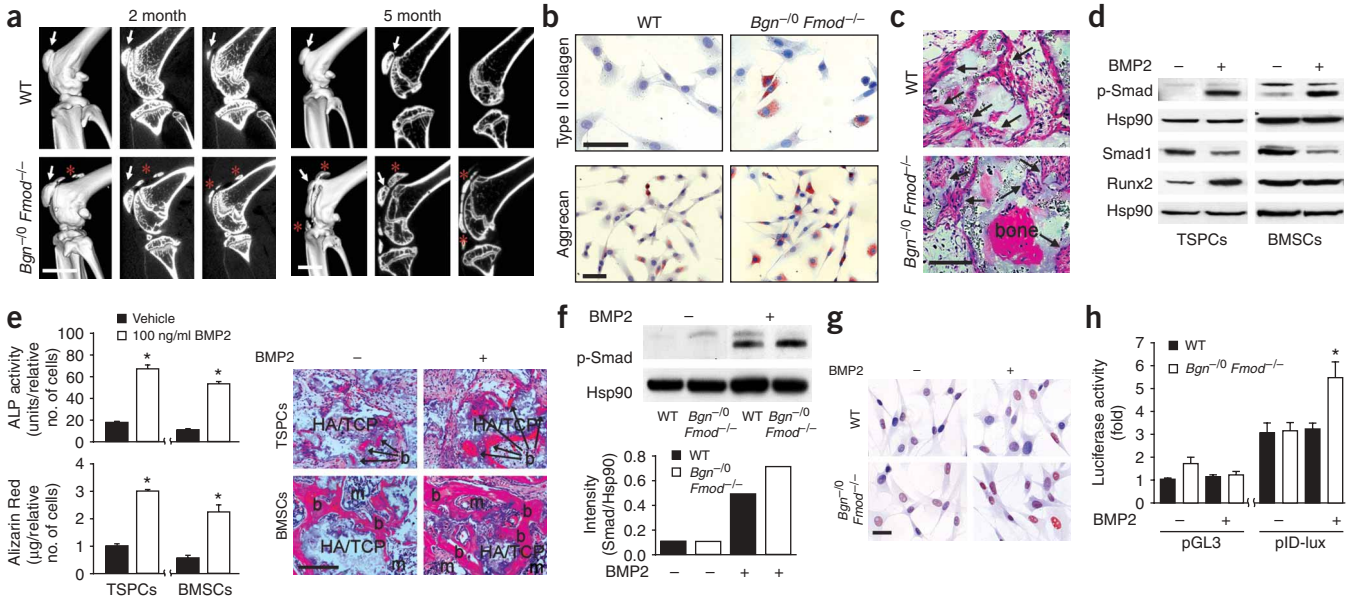

Figure 6 Ectopic activation of BMP signaling induces ossification in *Bgn*$^{-/0}$*Fmod*$^{-/-}$ mouse tendon tissue. (**a**) MicroCT image of the knees of 2- and 5-month-old *Bgn*$^{-/0}$*Fmod*$^{-/-}$ mice showed patellae (arrows) and ectopic ossicles (red asterisks) formed in tendons. Bars, 2 mm. (**b**) Immunocytochemistry staining of type II collagen and aggrecan in TSPCs from WT and *Bgn*$^{-/0}$*Fmod*$^{-/-}$ mice. Bar, 50 μm. (**c**) TSPCs from *Bgn*$^{-/0}$*Fmod*$^{-/-}$ mice form bone and tendon-like tissue (arrows) after *in vivo* transplantation. Bar, 100 μm. (**d**) Phosphorylation of Smad1-Smad5-Smad8 (faster migrating, lower bands) with or without BMP2 for 30 min (upper two panels) The upper band is nonspecific and is not induced by BMP. The expression of Smad1 and Runx2 with or without BMP2 for 10 d (lower three panels). Hsp90, loading control. (**e**) Alkaline phosphatase (ALP) activity (top left) and Ca^{2+} accumulation as judged by Alizerin Red staining (bottom left) in TSPCs and BMSCs with or without BMP2 for 3 d (upper) or 3 weeks (lower). Data are mean ± s.e.m. of three wells. $^*P < 0.0001$ vehicle versus BMP2. Bone formation, b, *in vivo* after cells were cultured with or without BMP2 for 2 weeks and then transplanted with HA/TCP into immunocompromised mice (right). Bone marrow (m). Bar, 200 μm. (**f**) BMP-induced phosphorylation of Smad1-Smad5-Smad8 in TSPCs from WT and *Bgn*$^{-/0}$*Fmod*$^{-/-}$ mice (top). A pan-pSmad antibody that recognizes phosphorylation of Smad1, Smad5 and Smad8 was used for pSmad detection. Hsp90, loading control. Densitometric analysis (bottom). (**g**) Nuclear localization of p-Smad1-Smad5-Smad8 in the presence or absence of BMP2 for 30 min. Bar, 50 μm. (**h**) The transcriptional activity of a reporter plasmid expressing a BMP-responsive luciferase construct (pID-lux). pGL3, control vector. The luciferase activity was reported as the fold increase over that of WT cells transfected with control vector in the absence of BMP2. Data are mean ± s.e.m. of three wells. $^*P < 0.02$ *Bgn*$^{-/0}$*Fmod*$^{-/-}$ versus WT.

was significantly higher in *Bgn*$^{-/0}$*Fmod*$^{-/-}$ TSPCs in the presence of BMP2 as compared to WT TSPCs (**Fig. 6h**). Taken together, these data indicate that BMP signaling was more active in the absence of both Bgn and Fmod.

DISCUSSION

We have successfully identified and isolated a unique cell population from human and mouse tendon tissues that, on the basis of a number of different criteria, shows characteristics of stem cells. With a DNA labeling-retention assay that has been used to identify putative stem cells in various tissues[31–33], we show that TSPCs reside within a niche environment that is surrounded predominantly by ECM proteins, thus suggesting that the ECM may play a major role in organizing the TSPC niche. Using mice deficient in the ECM proteins Bgn and Fmod, we provide evidence that the TSPC fate is controlled by specific components of this ECM-rich niche.

The isolation and characterization of TSPCs is important because the cells will provide a new tool to study basic tendon biology. Little is known about the factors that control tendon formation and maintenance, largely because tendon cells have been poorly characterized and because specific tendon markers have not been identified. One goal of our study was to identify such markers; for this we used a combination of RT-PCR, immunocytochemistry and FACS analyses. As is the case for other stem cells, no single marker could identify TSPCs; rather, a combination of factors must be used. Although TSPCs express many of the same markers as BMSCs, the expression patterns were not identical. TSPCs highly express tendon-related factors, such as Scx, TNMD, Comp and tenascin C. Mouse TSPCs expressed CD90.2, a fibroblast marker, but not CD18, a BMSC marker. These data suggest that TSPCs are closely related to BMSCs, but not identical.

The stem-cell niche has been defined as a specialized microenvironment that houses stem cells and maintains a balance of quiescence, self-renewal and cell-fate commitment. The stem-cell niche is a three-dimensional structure composed of cells, cytokines and the ECM[34,35]. A number of stem-cell niches have been identified within a variety of tissues and organs. For example, the osteoblasts govern the hematopoietic stem cell niche through the BMP, parathyroid hormone, and Tie2–angiopoietin-1 signaling pathways[10,11,36]. The bulge of the hair follicle, crypt and perivascular region provide niche microenvironments for epidermal, intestinal and neural stem cells, respectively, perhaps through multiple signaling pathways[12,37,38]. In addition, the perivascular region was also identified as the niche that maintains the 'stemness' of bone marrow stromal stem cells[13,14]. Although most of the identified niches are cell based, the ECM may also be involved in the regulation of stem cells. For example, ECM proteins, such as tenascin C, osteopontin and the combination of Bgn and decorin, have been found to control the number of neural stem cells, hematopoietic stem cells and BMSCs, respectively[27,39–42]. Given that tendon tissue is extremely rich in ECM components and contains substantially fewer cells than most tissues, we hypothesized that tendon tissue may contain a unique niche for TSPCs that is formed primarily by ECM

components. In this study, we show that the tendon stem-cell niche is composed predominantly of ECM and that alteration of ECM composition changes TSPC pool size; this detours TSPC fate from tenogenesis to osteogenesis, leading to ectopic ossification in the tendon of $Bgn^{-/0}Fmod^{-/-}$ mice.

ECM proteins (including proteoglycans) regulate the fate of stem cells within their niche by modulating the bioactivities of growth factors and cytokines to which ECM proteins often bind. In fact, tenascin C affects neuronal differentiation by modulating the sensitivity of the stem cells to fibroblast growth factor-2 and BMP4 (ref. 39). Our data also show increased sensitivity of TSPCs to BMP2 in the absence of Bgn and Fmod, which could be a mechanistic basis for altering the fate of TSPCs. BMP signaling has been shown to inhibit tendon formation during development[43]. In sum these observations reveal new and important roles for the ECM microenvironment in TSPC maintenance and ultimately in normal tissue development and maintenance.

The discovery of tendon stem cells that possess regenerative capabilities opens new possibilities for treating damaged tendon tissue that is slow to repair after injury. Unlike autologous bone grafts that can be harvested in large quantities from large bones like the pelvis, autologous tendon tissue is not readily available for use as grafting material. However, the ability to use small portions of tendons to isolate and expand cells that could form tendon tissue *in vivo* offers a new strategy for improving the current means of tendon repair. In addition, we show that TSPCs isolated from human tendons form tendon-like tissue and enthesis-like structures (bone-tendon junctions) when transplanted into immunocompromised mice. These data suggest that human TSPCs could eventually be used to treat patients with the damaged tendons or ruptured bone-tendon junctions (enthesopathies) that are commonly caused by tendon overuse or trauma.

A key limitation in using TSPCs to repair damaged tendon tissue is the availability of autologous tendon tissue. Previous studies indicated that BMSCs can form tendon- or ligament-type structures[44]. However, we show that BMSCs are different from TSPCs, and that they form bone rather than tendon-like tissue when *in vitro*–expanded cells are transplanted into mice. The repair and regeneration of tendon tissue with BMSCs without differential induction could potentially lead to ossification, thereby worsening the tendinopathy. Recent work shows that Smad8 overexpression in the immortalized BMSC-like cell line C3H10T1/2 induces tenogenic differentiation[45]. Finding the optimal conditions that will induce BMSC differentiation into tendon-forming cells will be crucial for the development of BMSC-based tendon repair. Given that tendon ECM controls tendon stem cell fate, it will be interesting to determine whether BMSCs will acquire tendon stem cell fate in the tendon ECM niche.

METHODS

Mice. We used male WT C57BL/6, C57BL/6-TgN(ACTbEGFP)1Osb mice (Jackson Labs), or $Bgn^{-/0}Fmod^{-/-}$ and their strain-matched WT mice (C57BL/6-129) with approval from the Animal Care and Use Committee, US National Institutes of Health (#NIDCR-DIR-05-347).

Cell isolation and culture. We obtained human hamstring tendon samples from individuals (age 8–12 years) that had undergone tenotomy to release hamstring contractures at Johns Hopkins University Hospital and followed the approved guidelines set by the US National Institutes of Health Office of Human Subjects Research (approval # OHSR 3005 for use of surgical waste). Mouse patellar tendons from 6–8-week-old mice were dissected as follows: we stripped off the tendon sheath and the surrounding paratenon, cut tendon tissues into small pieces and digested with 3 mg/ml collagenase type I (Worthington) and 4 mg/ml dispase (Roche) in PBS for 1 h at 37 °C. Single-cell suspensions were cultured in α-MEM (Gibco), supplemented with 20% lot-selected FBS (Equitech-Bio) and 100 mM 2-mercaptoethanol (Gibco) for 8–10 d at 5% CO_2, 37 °C. We also isolated and cultured bone BMSCs from the same individual or from the same mouse as previously described[46]. For assays of colony-forming efficiency, we cultured single-cell suspensions of tendon-derived cells in a 25-cm^2 flask for 9 d. We stained and scored the colonies and assessed the proliferation of TSPCs and BMSCs (passage 1) as previously described[27]. We calculated population doubling (PD) for each passage using the formula $PD \approx \log_2[N_c/N_o]$, where N_o is the inoculum cell population and N_c the number of cells at confluence, and added the PD from each passage together to obtain the population doubling values. We performed all the experiments with passage 1 for mouse TSPCs and passage 1 or 2 for human TSPCs.

Multipotent differentiation. We tested the *in vitro* multidifferentiation potential of the TSPCs toward osteogenesis, adipogenesis and chondrogenesis as described previously[27,47,48]. Osteogenic differentiation of TSPCs was quantified by the intensity of Alizarin Red S staining Ca^{2+} (ref. 49) and normalized to cell count using Cell Count Kit-8 (Dojindo). We visualized adipocytes using 0.3% Oil Red O (Sigma). We assessed chondrogenic differentiation of TSPCs by staining for toluidine blue and Safranin O or for type II collagen and aggrecan. We also examined the multidifferentiation potential of the TSPCs using an *in vivo* transplantation system as previously described[27,28], except TSPCs were first cultured *in vitro* in osteogenic induction medium for 2 weeks in the presence of 100 ng/ml BMP2 (Wyeth) before being mixed with HA/TCP (Zimmer).

Label-retaining cells. We injected BrdU (Sigma, 50 mg per g body weight) intraperitoneally into 3-d-old pups twice daily for 3 d. We detected BrdU-labeled cells on the paraffin-embedded sections using the BrdU Staining Kit (Zymed).

Western blotting. We treated confluent TSPCs or BMSCs with 100 ng/ml BMP2 or vehicle for the indicated times. The primary antibodies included rabbit-specific antibodies to phosphorylated Smad1 (p-Smad1), Smad1 (Cell Signaling, diluted 1:500), Hsp90 (Santa Cruz, diluted 1:500) and Aml-3 (Runx2) (Oncogene, diluted 1:100).

FACS analysis. We immunolabeled 5×10^5 cells with 1 μg of PE- or FITC-conjugated rat anti-mouse, mouse anti-human monoclonal antibodies or isotype-matched IgGs (**Supplementary Methods** online) for 1 h at 4 °C. For non-conjugated antibodies (**Supplementary Methods**), we incubated 1×10^6 cells with primary antibody for 1 h and fluorescent secondary antibody for 1 h at 4 °C, analyzed the samples using an Epics-XL-MCL flow cytometer (Beckman Coulter) and calculated data using the FACScan program (BD Biosciences).

RT-PCR. We designed primers (**Supplementary Methods**) with Primer3 software (http://www-genome.wi.mit.edu/cgi-bin/primer/primer3.cgi).

Nucleofection and luciferase reporter assays. We determined the activation of the BMP signaling pathway using the BMP-responsive luciferase reporter construct pID1–lux (ref. 50) as described in **Supplementary Methods**.

***In vivo* transplantation.** We mixed approximately $2–2.5 \times 10^6$ cells with 40 mg of HA/TCP ceramic powder (Zimmer), Gelfoam (3 mm × 3 mm × 2 mm, Pharmacia) or 50 μl Matrigel (BD Biosciences) subcutaneously onto calvariae or into the dorsal surface of 8–10-week-old female immunocompromised athymic nude-Foxn1nu mice (Harlan) as previously described[28]. We harvested the transplants 8-10 weeks later.

Histochemistry and immunohistochemistry. We histochemically stained paraffin-embedded sections with H&E, toluidine blue (Sigma), Safranin O (Sigma) or trichrome (Masson's or Goldner's). For immunohistochemical analysis, the sections were immunolabeled with primary antibodies (**Supplementary Methods**) at 25 °C for 1 h. Isotype-matched negative control antibodies (Zymed) were used under the same conditions. The broad-spectrum immunoperoxidase AEC kit (Picture Plus, Zymed) was subsequently used to detect the immunoactivity.

Immunocytochemistry. We fixed the transplant-derived TSPC colonies or passage 1 TSPCs with 4% paraformaldehyde in PBS at 25 °C for 20 min and immunostained with primary antibodies (**Supplementary Methods**) for 1 h at room temperature or overnight at 4 °C. The broad-spectrum immunoperoxidase AEC kit was subsequently used to detect the immunoactivity.

Microcomputed tomography analysis. We scanned and reconstructed mouse knees with 15 mm isotropic voxels on a microcomputed tomography analysis (μCT) system (eXplore MS, GE Medical Systems). The two-dimensional and three-dimensional images of the knee region were visualized with Microviewer (GE Medical Systems).

Statistical analysis. We reported representative data of at least three independent experiments. We performed statistical analyses with Student's *t*-test.

Note: Supplementary information is available on the Nature Medicine website.

ACKNOWLEDGMENTS

This research was supported in part by the Division of Intramural Research, US National Institute of Dental and Craniofacial Research, US National Institutes of Health and by an extramural grant from the US National Institutes of Health (US National Heart, Lung, and Blood Institute R01 HL61589-01 for L.Z.). We thank Å. Oldberg, University of Lund, Sweden for providing Fmod-deficient mice; P. Robey for advice and discussion on this work; H. Wimer, N. Marino, S. Kuznetsov and N. Cherman for technical assistance; and P. Vyomesh for his help with the isolation of mouse dermal fibroblasts.

AUTHOR CONTRIBUTIONS

Y.B. designed and performed the majority of the experiments, analyzed data and prepared the manuscript. D.E. performed, collected and analyzed the FACS data; T.M.K. maintained animals, assisted with *in vivo* experiments and collected tissue samples; C.A.I. performed nucleofection and luciferase reporter assays; M.C.E. and W.S. assisted with immunohistochemistry staining and L.L. prepared paraffin-embedded tissue sections. A.I.L. provided human samples. B.-M.S. helped with *in vitro* multipotent differentiation assays and *in vivo* transplantation. L.Z. designed the FACS analysis and helped with the preparation of the manuscript. S.S. designed the key experiments and prepared the manuscript. M.F.Y. performed RT-PCR and prepared the manuscript.

Published online at http://www.nature.com/naturemedicine
Reprints and permissions information is available online at http://npg.nature.com/reprintsandpermissions

1. Sharma, P. & Maffulli, N. Biology of tendon injury: healing, modeling and remodeling. *J. Musculoskelet. Neuronal Interact.* **6**, 181–190 (2006).
2. Kannus, P. Structure of the tendon connective tissue. *Scand. J. Med. Sci. Sports* **10**, 312–320 (2000).
3. Yoon, J.H. & Halper, J. Tendon proteoglycans: biochemistry and function. *J. Musculoskelet. Neuronal Interact.* **5**, 22–34 (2005).
4. Fenwick, S. *et al.* Endochondral ossification in Achilles and patella tendinopathy. *Rheumatology (Oxford)* **41**, 474–476 (2002).
5. Salingcarnboriboon, R. *et al.* Establishment of tendon-derived cell lines exhibiting pluripotent mesenchymal stem cell-like property. *Exp. Cell Res.* **287**, 289–300 (2003).
6. de Mos, M. *et al.* Intrinsic differentiation potential of adolescent human tendon tissue: an *in vitro* cell differentiation study. *BMC Musculoskelet. Disord.* **8**, 16 (2007).
7. Seo, B.M. *et al.* Investigation of multipotent postnatal stem cells from human periodontal ligament. *Lancet* **364**, 149–155 (2004).
8. Fuchs, E., Tumbar, T. & Guasch, G. Socializing with the neighbors: stem cells and their niche. *Cell* **116**, 769–778 (2004).
9. Taichman, R.S. & Emerson, S.G. Human osteoblasts support hematopoiesis through the production of granulocyte colony-stimulating factor. *J. Exp. Med.* **179**, 1677–1682 (1994).
10. Zhang, J. *et al.* Identification of the haematopoietic stem cell niche and control of the niche size. *Nature* **425**, 836–841 (2003).
11. Calvi, L.M. *et al.* Osteoblastic cells regulate the haematopoietic stem cell niche. *Nature* **425**, 841–846 (2003).
12. Shen, Q. *et al.* Endothelial cells stimulate self-renewal and expand neurogenesis of neural stem cells. *Science* **304**, 1338–1340 (2004).
13. Shi, S. & Gronthos, S. Perivascular niche of postnatal mesenchymal stem cells in human bone marrow and dental pulp. *J. Bone Miner. Res.* **18**, 696–704 (2003).
14. Doherty, M.J. *et al.* Vascular pericytes express osteogenic potential *in vitro* and *in vivo*. *J. Bone Miner. Res.* **13**, 828–838 (1998).
15. Brent, A.E., Schweitzer, R. & Tabin, C.J. A somitic compartment of tendon progenitors. *Cell* **113**, 235–248 (2003).
16. DiCesare, P.E., Morgelin, M., Mann, K. & Paulsson, M. Cartilage oligomeric matrix protein and thrombospondin 1. Purification from articular cartilage, electron microscopic structure, and chondrocyte binding. *Eur. J. Biochem.* **223**, 927–937 (1994).
17. Brandau, O., Meindl, A., Fassler, R. & Aszodi, A. A novel gene, tendin, is strongly expressed in tendons and ligaments and shows high homology with chondromodulin-I. *Dev. Dyn.* **221**, 72–80 (2001).
18. Spangrude, G.J., Heimfeld, S. & Weissman, I.L. Purification and characterization of mouse hematopoietic stem cells. *Science* **241**, 58–62 (1988).
19. Van Vlasselaer, P., Falla, N., Snoeck, H. & Mathieu, E. Characterization and purification of osteogenic cells from murine bone marrow by two-color cell sorting using anti–Sca-1 monoclonal antibody and wheat germ agglutinin. *Blood* **84**, 753–763 (1994).
20. Gussoni, E. *et al.* Dystrophin expression in the mdx mouse restored by stem cell transplantation. *Nature* **401**, 390–394 (1999).
21. Tamaki, T. *et al.* Identification of myogenic-endothelial progenitor cells in the interstitial spaces of skeletal muscle. *J. Cell Biol.* **157**, 571–577 (2002).
22. Welm, B.E. *et al.* Sca-1(pos) cells in the mouse mammary gland represent an enriched progenitor cell population. *Dev. Biol.* **245**, 42–56 (2002).
23. Miura, Y. *et al.* Defective osteogenesis of the stromal stem cells predisposes CD18-null mice to osteoporosis. *Proc. Natl. Acad. Sci. USA* **102**, 14022–14027 (2005).
24. Simmons, P.J. & Torok-Storb, B. Identification of stromal cell precursors in human bone marrow by a novel monoclonal antibody, STRO-1. *Blood* **78**, 55–62 (1991).
25. Filshie, R.J. *et al.* MUC18, a member of the immunoglobulin superfamily, is expressed on bone marrow fibroblasts and a subset of hematological malignancies. *Leukemia* **12**, 414–421 (1998).
26. Kuznetsov, S.A. *et al.* Single-colony derived strains of human marrow stromal fibroblasts form bone after transplantation in vivo. *J. Bone Miner. Res.* **12**, 1335–1347 (1997).
27. Bi, Y. *et al.* Extracellular matrix proteoglycans control the fate of bone marrow stromal cells. *J. Biol. Chem.* **280**, 30481–30489 (2005).
28. Krebsbach, P.H. *et al.* Bone formation *in vivo*: comparison of osteogenesis by transplanted mouse and human marrow stromal fibroblasts. *Transplantation* **63**, 1059–1069 (1997).
29. Bickenbach, J.R. Identification and behavior of label-retaining cells in oral mucosa and skin. *J. Dent. Res.* **60**, 1611–1620 (1981).
30. Ameye, L. *et al.* Abnormal collagen fibrils in tendons of biglycan/fibromodulin-deficient mice lead to gait impairment, ectopic ossification, and osteoarthritis. *FASEB J.* **16**, 673–680 (2002).
31. Cotsarelis, G., Sun, T.T. & Lavker, R.M. Label-retaining cells reside in the bulge area of pilosebaceous unit: implications for follicular stem cells, hair cycle, and skin carcinogenesis. *Cell* **61**, 1329–1337 (1990).
32. Morris, R.J. & Potten, C.S. Slowly cycling (label-retaining) epidermal cells behave like clonogenic stem cells in vitro. *Cell Prolif.* **27**, 279–289 (1994).
33. Booth, C. & Potten, C.S. Gut instincts: thoughts on intestinal epithelial stem cells. *J. Clin. Invest.* **105**, 1493–1499 (2000).
34. Scadden, D.T. The stem-cell niche as an entity of action. *Nature* **441**, 1075–1079 (2006).
35. Krause, D.S. Regulation of hematopoietic stem cell fate. *Oncogene* **21**, 3262–3269 (2002).
36. Arai, F. *et al.* Tie2/angiopoietin-1 signaling regulates hematopoietic stem cell quiescence in the bone marrow niche. *Cell* **118**, 149–161 (2004).
37. Moore, K.A. & Lemischka, I.R. Stem cells and their niches. *Science* **311**, 1880–1885 (2006).
38. Blanpain, C. & Fuchs, E. Epidermal stem cells of the skin. *Annu. Rev. Cell Dev. Biol.* **22**, 339–373 (2006).
39. Garcion, E., Halilagic, A., Faissner, A. & Ffrench-Constant, C. Generation of an environmental niche for neural stem cell development by the extracellular matrix molecule tenascin C. *Development* **131**, 3423–3432 (2004).
40. Nilsson, S.K. *et al.* Osteopontin, a key component of the hematopoietic stem cell niche and regulator of primitive hematopoietic progenitor cells. *Blood* **106**, 1232–1239 (2005).
41. Ohta, M., Sakai, T., Saga, Y., Aizawa, S. & Saito, M. Suppression of hematopoietic activity in tenascin-C–deficient mice. *Blood* **91**, 4074–4083 (1998).
42. Stier, S. *et al.* Osteopontin is a hematopoietic stem cell niche component that negatively regulates stem cell pool size. *J. Exp. Med.* **201**, 1781–1791 (2005).
43. Schweitzer, R. *et al.* Analysis of the tendon cell fate using Scleraxis, a specific marker for tendons and ligaments. *Development* **128**, 3855–3866 (2001).
44. Awad, H.A. *et al.* Autologous mesenchymal stem cell–mediated repair of tendon. *Tissue Eng.* **5**, 267–277 (1999).
45. Hoffmann, A. *et al.* Neotendon formation induced by manipulation of the Smad8 signalling pathway in mesenchymal stem cells. *J. Clin. Invest.* **116**, 940–952 (2006).
46. Kuznetsov, S.A., Friedenstein, A.J. & Robey, P.G. Factors required for bone marrow stromal fibroblast colony formation *in vitro*. *Br. J. Haematol.* **97**, 561–570 (1997).
47. Gimble, J.M. *et al.* Bone morphogenetic proteins inhibit adipocyte differentiation by bone marrow stromal cells. *J. Cell. Biochem.* **58**, 393–402 (1995).
48. Johnstone, B., Hering, T.M., Caplan, A.I., Goldberg, V.M. & Yoo, J.U. *In vitro* chondrogenesis of bone marrow–derived mesenchymal progenitor cells. *Exp. Cell Res.* **238**, 265–272 (1998).
49. Kostenuik, P.J., Halloran, B.P., Morey-Holton, E.R. & Bikle, D.D. Skeletal unloading inhibits the *in vitro* proliferation and differentiation of rat osteoprogenitor cells. *Am. J. Physiol.* **273**, E1133–E1139 (1997).
50. Lopez-Rovira, T., Chalaux, E., Massague, J., Rosa, J.L. & Ventura, F. Direct binding of Smad1 and Smad4 to two distinct motifs mediates bone morphogenetic protein–specific transcriptional activation of Id1 gene. *J. Biol. Chem.* **277**, 3176–3185 (2002).